JOURNAL OF CATALYSIS 99, 117–125 (1986)

Hydrothermal Dealumination of Faujasites

T. H. FLEISCH,* B. L. MEYERS,* G. J. RAY,* J. B. HALL,* AND C. L. MARSHALL†

* *Analytical Research and Services Division, Amoco Corporation; and †Research and Development Department, Amoco Oil Company, Amoco Research Center, P.O. Box 400, Naperville, Illinois 60566*

Received July 29, 1985; revised December 12, 1985

Two faujasites (USY and REY) were hydrothermally treated at temperatures between 400 and 850°C in 100% steam and up to 65 h to induce dealumination. The Al expulsion from the zeolite lattice was followed by X-ray diffraction (XRD) and by ^{29}Si and ^{27}Al nuclear magnetic resonance (NMR) spectroscopy. Both techniques showed large changes in crystal structure in less than 30 min while crystallinity lossses were kept below 15% at temperatures up to 500°C. Excellent agreement in the rate of dealumination was found between XRD and ^{29}Si NMR measurements. The Al expulsion from the zeolite lattice is accompanied by Al diffusion through the channel network to the zeolite particle surface. The surface enrichment by Al was quantitatively measured by X-ray photoelectron spectroscopy (XPS or ESCA). The dealumination and Al migration processes are both logarithmic with time and a linear correlation between them was found at all temperatures for up to 65 h of steaming. The diffusion of Al to the particle surface takes place only in the presence of steam and the migrating species is speculated to be a hydroxylated Al ion. These studies were complemented by secondary ion mass spectrometry (SIMS) and scanning transmission electron microscopy (STEM). SIMS analysis demonstrated a very large enrichment of Al in the top 30 Å of steamed zeolites. STEM measurements of Si/Al profiles on 800 Å-thick microtomed sections confirmed the SIMS data, but indicated broader, less steep changes in the Si/Al ratio across zeolite particles. Because dealumination causes both structural changes (shrinkage of unit cell) and chemical changes (decrease in acidity) in a zeolite, it has profound implications on catalyst performance and on catalyst deactivation. For instance, dealuminated faujasites exhibit drastically reduced coking rates in the cumene cracking test reaction which will be discussed in some detail.

INTRODUCTION

The dealumination of zeolites in general and of faujasites in particular is a well known process which was first reported over 20 years ago (*1*). An excellent review on this subject was recently written by Scherzer (*2*). There are several different ways to accomplish zeolite dealumination. Among the chemical methods are treatments with acids, e.g., HCl (*1*, *3–5*), with volatile halides, e.g., $SiCl_4$ (*6*), or with chelating agents such as EDTA (*7–9*). The most commonly used technique, however, is a hydrothermal treatment of the zeolite in either pure steam or air/steam mixtures (*10–15*).

The work presented in this paper will focus on the hydrothermal dealumination of two faujasites, USY and REY (Rare Earth exchanged Y), in pure steam between 400 and 500°C. The expulsion of Al from the framework has been measured by x-ray diffraction (XRD) and by ^{29}Si nuclear magnetic resonance (NMR) spectroscopy. Under the hydrothermal dealumination conditions the expelled, nonframework Al migrates through the channel network to the crystallite surfaces resulting in Al enriched surfaces (*16*, *17*). This Al migration to the surface has been studied by X-ray photoelectron spectroscopy (XPS), secondary ion mass spectrometry (SIMS), and by scanning transmission electron microscopy (STEM). A novel correlation between dealumination as measured by XRD and Al surface segregation as measured by XPS has been established. The changes in the catalytic performance due to dealumination were followed by a cumene cracking test reaction. The results indicate that the tendency of Al ions to form coke decreases

0021-9517/86 $3.00

rapidly as they become more isolated in the zeolite framework.

EXPERIMENTAL

Sample Preparation

Ultrastable-Y (USY) was prepared from Davison Z-14 US zeolite. One thousand grams of Z-14 was slurried with 4000 ml of a 1.4 *M* NH_4HO_3 solution at 60°C for 1 h, filtered, and then reslurried with fresh NH_4NO_3 solution. This procedure was repeated three times. The final zeolite was dried *in vacuo* at 100°C overnight and calcined at 750°C for 4 h. Elemental analysis of the final USY showed 0.46 wt% residual sodium.

The rare earth chloride zeolite was prepared from SK-40 grade Y zeolite (Union Carbide). A slurry of 3000 g of the zeolite was heated to reflux temperature in 8 liters of distilled water. To this was added 4000 g of a mixed rare earth chloride solution (Davison Chemical Co., ~15 wt% rare earths in water). The slurry was refluxed with stirring for 1 h, filtered, then refluxed again in a fresh solution of rare earth chloride. As was done for the US-Y this procedure was repeated three times in order to assure complete exchange of the zeolite. The sample was then dried *in vacuo* at 120°C overnight and calcined at 750°C for 4 h in flowing air. Elemental analysis of the calcined product showed 0.24 wt% residual sodium.

Fixed Bed Steamings

Fixed bed steaming of all materials was done in an up-flow quartz tube reactor (20 mm o.d.) in a 100% steam atmosphere. Three grams of the material is loaded into the reactor (35–50 mm bed depth) and the temperature brought up to the appropriate steaming temperature in flowing nitrogen. Distilled water was then metered into the bottom of the reactor for the appropriate amount of time. All samples were then analyzed without further washings or calcination.

XRD

Prior to X-ray diffraction measurements, samples were dried at 100°C and then equilibriated at 35% humidity in a desiccator containing saturated $CaCl_2 \cdot 6H_2O$. Measurements were made on a Phillips Electronics diffractometer. A curved graphite crystal monochromator was employed with a high-intensity fine focus copper X-ray source. NaCl was used as an internal standard and a_0 (the cubic lattice edge) was calculated from the average of six reflections of known Miller indices in the 45–57° 2θ range. These measurements are accurate to better than 0.01 Å. Relative zeolite crystallinity was measured by determining the integrated intensity of the 533 peak after equilibration of the sample in 35% humidity atmosphere. Starting materials were assumed to be 100% crystalline.

XPS

The sample surfaces were analyzed in a Hewlett–Packard 5950B electron spectrometer. The sample powders were pressed into 6-mm-diameter pellets with a thickness of approximately 1 mm, which, in turn, were put into sample holders. Monochromatic Al$K\alpha$ ($h\nu$ = 1486.6 eV) radiation was used providing linewidths on the order of 0.80 eV FWHM for the Au $4f_{7/2}$ photoelectron line. A 2- × 8-mm section of the sample surface is analyzed. Sample charging was minimized by the use of an HP electron flood gun which produces low-energy electrons (<5 eV) to the sample surface during XPS analysis. The binding energy scale was calibrated by assigning a binding energy of 103.5 eV to the Si 2*p* photoelectron peak. Elemental concentrations were calculated after correcting Si 2*p* Al 2*p*, O 1*s*, and C 1*s* peak areas for instrumental parameters, differences in photoionization cross section, and differences in electron mean free path.

SIMS

The SIMS experiments were performed in a PHI 550 instrument equipped with a

SIMS II unit. An Ar ion beam with 2 keV energy was used as excitation source. The ion current density was adjusted to a level where the sputter rate of Pt of evaporated Pt films was 15 Å/min. This procedure allowed the acquisition of the experimental data (Al^+ and Si^+ peak heights) in a time period where only a small fraction of a monolayer was removed. As in the XPS experiments, an electron beam had to be employed to avoid sample charging.

NMR

^{29}Si NMR spectra were obtained on a Nicolet NT-300 spectrometer which operated at 7.05 T and was equipped with a broadband Chemagnetics MAS probe. A spectral width of 10 kHz was acquired in 512 data points which were zero-filled to 2 K after using a Gaussian line broadening of 100 Hz. An 8.5 μs (45°) excitation pulse, 2.0 s relaxation delay and 2000 acquisitions were used. ^{29}Si chemical shifts were referenced to TMS by using an external sample of HMDS which has a chemical shift of 6.7 ppm from TMS. Bullet rotors with an internal diameter of 7 mm and a height of 12 mm were used and spinning rates were between 3 and 5 kHz.

STEM

Thin sections of the sample were analyzed in a Philips 400T scanning transmission electron microscope (STEM) equipped with a Tracor Northern 2000 energy-dispersive X-ray analyzer (EDX). The thin sections were prepared by dispersing the sample particles in epoxy and cutting sections with an ultramicrotome. Sections less than about 900 Å thick were mounted for analysis. The Al/Si ratio was determined at several locations across each particle cross section. The electron probe (~100 Å diameter) was positioned at each location and the net Al and Si X-ray counts were measured. The ratio of these net counts was used as a measure of the Al/Si atomic ratio for each point.

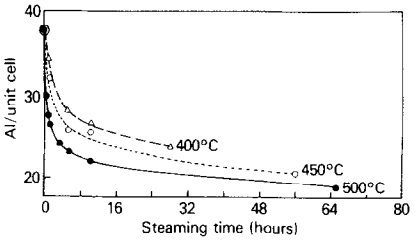

FIG. 1. Changes in Al content for USY as a function of steaming time to 400, 450, and 500°C as measured by XRD.

Cumene Cracking

Zeolite activity measurements were determined using a microbalance reactor system with cumene (isopropylbenzene) as the probe feed. The system uses a Cahn 2000 microbalance set on the 1-mg sensitivity range and connected to a strip chart recorder. The reactor is a gold mesh basket in which 50 mg of the zeolite is placed. After precalcination in air at 575°C the reactor is cooled to 500°C in flowing He until a baseline is established. Cumene is then introduced into the reactor by bubbling He through cumene at 0°C. Coke buildup on the catalyst is recorded by the microbalance as an increase in catalyst weight. The amount of cumene conversion is determined by an on-line GC, sampling the gas stream every 10 min.

RESULTS AND DISCUSSION

Aluminum Expulsion

The untreated USY zeolite has a unit cell dimension of 24.53 Å which can be translated into an Al/Si atomic ratio of 0.26 corresponding to 39 Al per unit cell. Upon dealumination the unit cell shrinks because of Si—O bonds (1.61 Å) replacing longer Al—O bonds (1.74 Å). The decrease in unit cell is 0.00868 Å per Al. Figure 1 shows the decrease in the number of Al per unit cell as calculated from the unit cell shrinkage measured by XRD as function of steaming time at 400, 450, and 500°C. At the latter temperature, the number of Al per unit cell decreases from 39 to 19 after 65 h of steaming.

TABLE 1

Crystallinity Loss and Changes in Unit Cell Dimension (A_0) of USY upon Steaming at 500°C

Steaming time (h)	Crystallinity loss (%)	A_0 (Å)
0	—	24.55
0.5	14	24.45
1	17	24.43
3	17	24.41
5	17	24.40
10	17	24.39
65	17	24.36

Most of the dealumination occurs in a very short time. A close look at the early part of this curve shows that about half of dealumination occurs in the first 30 min. Aluminum extraction from the framework structure is so rapid and extensive in this short period of time that there is approximately a 15% loss in crystallinity. This is undesirable but is the price one pays for rapid, extensive dealumination. Crystallinity loss can be minimized by steaming at lower temperatures or by using lower steam concentrations.

Nearly all of the crystallinity loss occurs during the first 30 min when the dealumination is very rapid as shown in Table 1 for USY steamed at 500°C. It appears that there is not enough time to fill the hole left by an expelled Al with a Si ion before the crystalline structure falls apart. Furthermore, the lack of "casual" Si to heal the structure might be another important contributing factor. After the destruction of a few percents of the zeolite there is a good source of "casual" Si to fill the dealuminated sites (*13, 23*). Thus, the absence of any further crystallinity losses at prolonged steaming times between 400 and 500°C is probably the result of both slower dealumination rates and availability of "casual" Si.

Silicon NMR spectroscopy has also been used to follow dealumination (*18, 19*). The ^{29}Si MAS NMR spectra of samples USY that have been subjected to steaming for various lengths of time are shown in Fig. 2. Each spectrum consists of four peaks that occur at chemical shifts of −90.2, −95.5, −101.8, and −107.5 ppm and which have been assigned to silicon in the environment $Si(OAl)_n(OSi)_{4-n}$ where n equals 3,2,1, and 0, respectively (*18*). Because of the low Al concentration in USY only a few Si sites have three Al neighbors. No Si sites with four Al neighbors could be detected. The removal of Al from the framework results in an increase in the intensity of Si sites with no Al neighbors. The calculation of Al contents after curve-fitting of these data yields Al concentrations that agree very well with XRD data (*20*). Thus, dealumination of sieves can be quantitatively measured by two independent techniques. NMR has the advantage of providing additional short range structural information such as the distribution of Si sites with 0,1,2,3, or 4 nearest Al neighbors (*18*). Such data can be very important catalytically because different sites probably have different catalytic properties and almost certainly have different thermal stabilities.

Aluminum Ion Migration

So far the expulsion of Al from the zeolite framework has been discussed. Now attention is focussed onto the Al ion migration. Our results indicate that hydroxylated

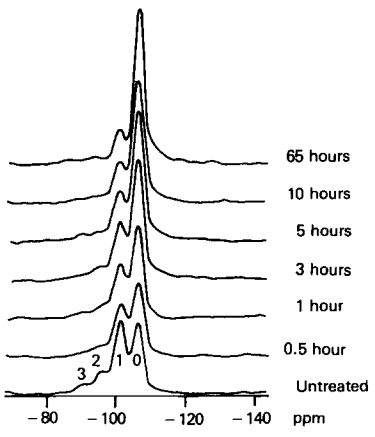

FIG. 2. ^{29}Si MAS NMR spectra of USY zeolite as a function of steaming time at 500°C.

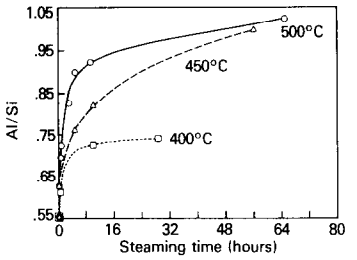

FIG. 3. Changes in Al/Si surface atomic ratios in USY as a function of steaming time at 400, 450 and 500°C as measured by XPS.

Al ions are formed and that they rapidly migrate through the channels and eventually concentrate on the outer surface of the zeolite particle. This Al ion migration was studied by XPS, SIMS, and STEM. The enrichment of Al on the zeolite particle surfaces expressed as Al/Si atomic ratio is shown in Fig. 3 as function of steaming time. The same samples as analyzed by XRD (Fig. 1) were studied. As was shown with XRD data, there are very rapid initial changes during steaming. The unsteamed catalyst has an Al/Si ratio of 0.55. But at 500°C this ratio increases to 0.7 after 1 h and to slightly over 1 after 65 h. The surface Al enrichment curves seem to mirror the changes observed in the bulk by XRD (Fig. 1).

The shape of the curves indicated an exponential dependence on steaming time. Indeed, the Al/Si atomic ratio changes logarithmically with steaming time as shown by the semilog plot in Fig. 4. The same logarithmic dependence as for USY has been found for REY. In the latter case the Al/Si surface atomic ratio increases to 0.56 and 0.77 after 0.5 and 64 h of steaming at 500°C, respectively (Fig. 4). The higher Al/Si ratios of USY compared to REY is at first surprising since it is opposite to the bulk ratios but it can be easily rationalized. The Al/Si surface atomic ratio of REY is 0.53 and is very close to the calculated bulk value of 0.48. Thus, only a very modest Al surface enrichment, if any, is observed on the untreated REY surface. The Al/Si surface atomic ratio of untreated USY, on the other hand, is 0.55 which is a factor of 2 higher than the bulk value of 0.26. Amorphous alumina originating from the hydrothermal preparation of USY from Y zeolite is present on the USY surface. Thus, the Al signal detected by XPS arrives from both structural and nonframework Al. The latter one can be removed by mild acid washing. Figure 4 shows the large drop in the Al/Si ratio of USY after a wash in 0.1 *N* HCl at room temperature due to the partial removal of amorphous alumina. XRD analyses showed no change in the unit cell dimension alluding to the absence of any framework dealumination by this acid treatment.

Not only the Al surface enrichment is logarithmic with time but also the dealumination itself. This is demonstrated for the steaming of REY at 500°C. In Fig. 5, we have plotted changes in unit cell on the left-hand ordinate and changes in the Al/Si surface atomic ratio on the right-hand ordinate as function of steaming time. Both processes are logarithmic with time and there is a very good correlation between these two measurements. This correlation is remarkable since XRD as a bulk technique follows dealumination at the atomic level

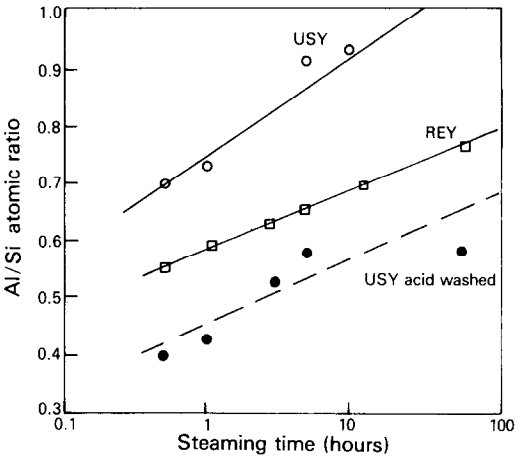

FIG. 4. Changes of Al/Si atomic ratios in USY and REY upon steaming at 500°C. Removal of nonframework Al in steamed USY by acid washing (0.1 *N* HCl).

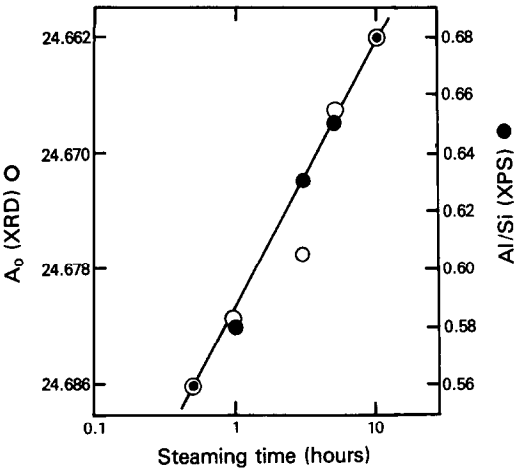

FIG. 5. Correlation of dealumination and Al surface enrichment during the first 10 h of steaming of REY at 500°C.

while XPS as a surface sensitive technique measures the Al in the top 40 Å of the zeolite particle. These data clearly demonstrate that there is a relationship between zeolite dealumination and subsequent aluminum migration to the surface.

This relationship is shown in a slightly different way in Fig. 6. Here we have linearly plotted changes in unit cell by XRD versus the Al/Si surface ratio by XPS. Thus we show the first 30 min of dealumination which could not be shown in the previous semilog plot. A first discontinuity in this relationship occurs at about one-half hour. Approximately as much dealumination occurs in this period of time as in the following 64 h. On the other hand, the Al surface enrichment is relatively small in this time period. Arrival of Al at the surface lags dealumination at first, but the two processes soon reach a steady state. Several explanations can be offered for the shape of this plot. The initial rapid dealumination could simply result from the unstable nature of Al-rich sites. Another explanation is that dealumination is actually dependent upon migration of the expelled Al through the sieve channels to the surface. This could explain the initial rapid dealumination which soon becomes inhibited by the presence of expelled Al in the channels. The rate of Al migration to the surface thus becomes the limiting factor producing the steady state. This speculation is supported by other studies of ours which show that in the absence of steam there is no Al migration, and only very limited dealumination. Aluminum migration induced by steam or Al removal by acid treatment or some other measure appears to be necessary for extended dealumination.

A second discontinuity at very long steaming times, also shown in Fig. 6, supports the suggested mechanism. While the dealumination comes to a halt, Al migration continues through the channel network to the particle surfaces. This third regime in the crossplot of dealumination and Al arrival at the surface was not seen in an otherwise identical relationship for USY reported by us previously (*21*). For USY the steady-state relationship continued throughout the 65 h of steaming of 500°C and longer times would have been needed to reach the point of the second discontinuity. The earlier halt of dealumination in REY is due to the framework stabilization by the rare earths.

The Al ion migration to the surface was also studied by SIMS. Every few seconds a spectrum between 22 and 32 amu was collected while the surface was etched with a rate of about 5 Å per minute. This sputter

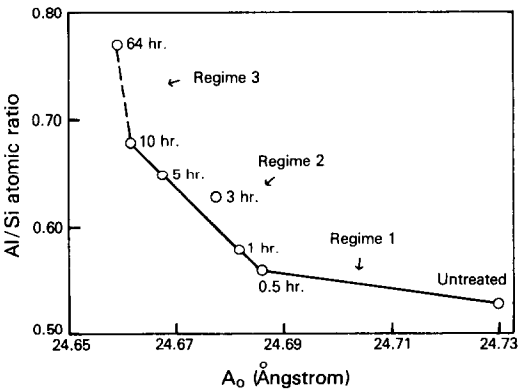

FIG. 6. Correlation of Al/Si surface atomic ratios and A_0 of REY zeolite after steaming at 500°C.

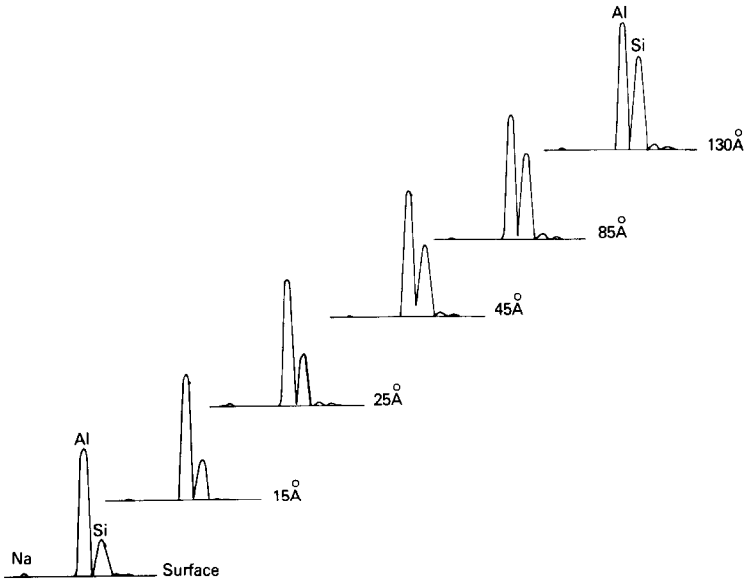

FIG. 7. Changes in positive-ion SIMS spectra as a function of sample depth.

rate was obtained by correcting the measured and calibrated sputter rate of Pt for the sputter rate of SiO_2 (*22*). The latter is the closest compound to a faujasite for which sputter rates have been measured. Figure 7 compares a sequence of positive ion SIMS spectra from different depths of the USY zeolite, steamed at 500°C for 65 h. It is quite obvious that the Al/Si peak height ratio (Al = 27, Si = 28) changes drastically as function of depth with much higher Al concentrations on the outermost layers. The other peaks in this mass range indicate Na^+ (23 amu) and Si^+ isotopes (29 and 30 amu).

The Al/Si peak height ratio has been plotted as function of Ar ion bombardment time in Fig. 8. The untreated USY zeolite already has an Al concentration gradient within the first 50 Å in agreement with the XPS data. The Al/Si peak height ratio decreases from 2.2 in the first 2 to 4 Å to 1.2 at a depth of about 60 Å. After a washing with 0.1 *N* HCl at room temperature, with most of the amorphous alumina removed, a nearly uniform Al/Si ratio is observed (*16*). After 65 h of steaming the Al/Si ratio on the top surface has increased to about 3.6 but drops rapidly to about 1.5 after 12 min of Ar ion bombardment. The Al that has migrated to the surface can be removed by acid washing as shown in Fig. 8. These SIMS data are in excellent agreement with a fast atom bombardment mass spectrometry (FABMS) study by Dwyer *et al.* (*16, 17*). They found Al surface enrichment in steamed faujasites, mordenites, and ZSM-5

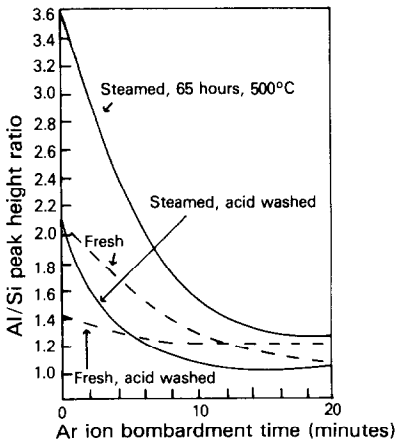

FIG. 8. Changes in SIMS Al/Si peak height ratio as a function of sample depth (Ar ion etching). Differences in Al concentration gradients among untreated, dealuminated, and acid-washed USY zeolites.

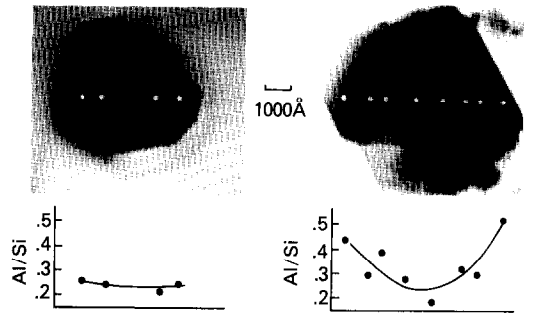

FIG. 9. STEM micrographs and EDX Al/Si ratios of fresh and dealuminated USY zeolite.

as well as Al surface removal following treatment with acidic solutions.

Conversion of the Al/Si peak height ratio into a quantitative Al/Si atomic ratio is not possible because no data of sputter rates and ionization probabilities of Al and Si in a USY zeolite are known. However, because of the chemical similarity of Al and Si, these numbers should be very similar for both elements. Indeed, sputter rates within a factor of 2 have been reported for SiO_2 and Al_2O_3 (*22*) and secondary ion yields within a factor of 1.5 for Si and Al (*22*). Thus, the Al/Si peak height ratios without any correction should be within about a factor of 3 of the atomic ratios. Indeed, a comparison of the SIMS Al/Si peak height ratios with quantitative Al/Si atomic ratios shows that a division of the SIMS peak height ratios by about 3.5 yields Al/Si atomic ratios that agree well with other measurements.

A third independent measurement of Al ion migration throughout zeolite particles was performed with STEM/EDX. Figure 9 shows electron micrographs of cross sections of particles of fresh USY and USY steamed for 65 h at 500°C. The particles shown are enlarged 100,000 times. At each of the indicated points across the particle, Si and Al were measured. These analyses describe the average composition of a volume about 100 Å in diameter and 800 Å thick. The Al/Si atomic ratios are plotted on the same scale and shown in the lower part of Fig. 9. The fresh sample shows almost a constant Al/Si ratio across the section. The steamed sample again shows large enrichments in Al toward the particle surface and thus supports the migration of Al from the particle framework through the channel network to outside surface. The point-to-point fluctuations in data are reproducible and are probably due to internal inhomogeneities, grain boundaries, and other internal structures.

Catalytic Implications

The effect of dealumination on catalytic properties is illustrated in Figs. 10 and 11. In the former one the cumene cracking activity during the first 200 min on-stream is compared for the untreated and 65 h/500°C steamed USY zeolite. The untreated zeolite with about 30 Al/unit cell exhibits high initial activity but suffers a rapid activity decline. The dealuminated USY with 19 Al/unit cell is initially less active but deactivates much more slowly. The difference in the initial activity is expected since cracking occurs on the highly acidic Al sites. The difference in the deactivation behavior can be understood from the extent of coking shown in Fig. 10b. The Al-rich zeolite lays down coke at 5 to 6 times the rate as the dealuminated zeolite. The coke plugs the pores which inhibits the diffusion of cumene to the active site. This extensive coke

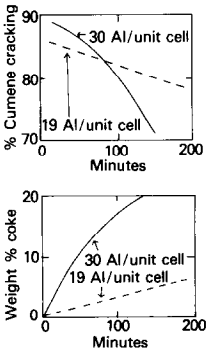

FIG. 10. Cumene cracking activity and coke formation for untreated and dealuminated USY zeolite as function of reaction time.

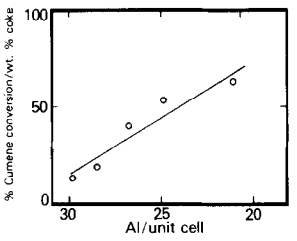

FIG. 11. Selectivity of USY zeolites as a function of Al content.

buildup on the aluminum rich zeolite explains its very rapid deactivation. Bremer *et al. (24)* also found lower coke yields in the cracking of gas oils over dealuminated faujasites as compared to REY faujasites.

The coking data were used to calculate a selectivity factor. The selectivity factor is obtained by dividing the weight percent conversion at 30 min on stream by the weight percentage of coke at the same time. The higher the number, the more selective the catalyst is to the more desirable cracking reactions. Figure 11 shows that the selectivity toward useful products increases linearly with decreasing Al content. It implies that as Al ions become more isolated in the zeolite framework their tendency to coke decreases. This relationship illustrates the practical implications of dealumination studies.

CONCLUSIONS

Steam treatments of zeolites leads to the expulsion of Al from the framework. This dealumination can be quantitatively measured by XRD and ^{29}Si NMR. The expelled Al migrates to and accumulates on the surface of the zeolite particles as evidenced by XPS, SIMS, and STEM/EDX measurements. Both, the dealumination and Al ion migration are logarithmic with time and can be linearly correlated over extended steaming periods. Dealuminated zeolites exhibit decreased coking tendency and improved selectivities.

REFERENCES

1. Barrer, R. M., and Makki, M. B., *Canad. J. Chem.* **42,** 1481.
2. Scherzer, J., *ACS Symp. Ser.* **248,** 157 (1986).
3. Breck, D. W., Eversole, W. G., Eversole, R. M., Milton, R. M., Reed, T. B., and Thomas, T. L., *J. Amer. Chem. Soc.* **78,** 5964 (1956).
4. Frilette, V. J., and Rubin, M. K., *J. Catal.* **4,** 310 (1965).
5. Eberly, P. E., Jr., and Kimberlin, C. N., Jr., *Ind. Eng. Chem. Prod. Res. Dev.* **9,** 335 (1970).
6. Beyer, H. K., and Belenykaja, I., *in* "Catalysis by Zeolites" 203, (B. Imelik, Ed.), p. 203. Elsevier, Amsterdam, 1980.
7. Kerr, G. T., *J. Phys. Chem.* **73,** 2780 (1969).
8. Kerr, G. T., *J. Phys. Chem.* **72,** 2594 (1968).
9. Kerr, G. T., Chester, A. W., and Olson, D. H., *Acta Phys. Chem.* **24,** 169 (1978).
10. McDaniel, C. V., and Maher, P. K., Conf. Mol. Sieves, 1967, Soc. of Chem. Ind., London, Monogr. 186 (1968), U.S. Patent 3,293,192 (Dec. 20, 1966).
11. Kerr, G. T., *J. Catal.* **15,** 200 (1969).
12. Ward, J. W., *J. Catal.* **18,** 348 (1970).
13. Maher, P. K., Hunter, F. D., and Scherzer, J., *Adv. Chem. Ser.* **101,** 266 (1971).
14. Peri, J. B., *in* "Proceedings, 5th International Congress on Catalysis, Palm Beach, 1972" (J.W. Hightower, Ed.), p. 329. North-Holland, Amsterdam, 1973.
15. Uytterhoeven, J. B., Christer, L. G., and Hall, W. K., *J. Phys. Chem.* **69,** 2117 (1969).
16. Dwyer, J., Fitch, F. R., Machado, F., Qin, G., Smyth, S. M., and Vickerman, J. C., *J. Chem. Soc. Commun.*, 422 (1981).
17. Dwyer, J., Fitch, F. R., Qin, G., and Vickerman, J., *J. Phys. Chem.* **86,** 4574 (1982).
18. Klinowski, J., Ramdas, S., Thomas, J. M., Fyfe, C. A., Hartman, J. S., *J. Chem. Soc., Faraday Trans. 2* **78,** 1025 (1982).
19. Klinowski, J., Thomas, J. M., Fyfe, C. A., and Gobbi, G. C., *Nature (London)* 296, 533 (1982).
20. Ray, G. J., Meyers, B. L., and Marshall, C. L., submitted for publication.
21. Meyers, B. L., Fleisch, T. H., and Marshall, C. L., *Appl. Surf. Sci.*, in press.
22. Perkin–Elmer, Physical Electronics Division, Handbook of SIMS.
23. Lohse, U., Stach, H., Thamm, H., Schirmer W., Isirikjan, A. A., Regent, N. L., and Dubinin, M. N., *Z. Anorg. Allg. Chem.* **460,** 179 (1980).
24. Bremer, H., Lohse, U., Reschetilowski, W., and Wendland, K. P., *Z. Anorg. Allg. Chem.* **482,** 235 (1981).